

AN EXPERIMENTAL STUDY OF CRITICAL HEAT FLUX FOR LOW FLOW OF WATER IN VERTICAL ROUND TUBES UNDER LOW PRESSURE

Won-Pil Baek, Jae Wook Park and Soon Heung Chang
Department of Nuclear Engineering
Korea Advanced Institute of Science and Technology
373-1 Kusong-dong, Yusong-gu, Taejon, 305-701, Korea
(TEL) 82-42-869-3816 (FAX) 82-42-869-3810

ABSTRACT

An experimental study has been performed on the critical heat flux (CHF) for stable low flow of water in vertical round tubes under low pressure. Experiments have been performed with a test section of diameter 0.01m (heated length = 0.9 and 0.6m) under atmospheric pressure. Test results are discussed in the aspects of parametric effects of the following parameters: mass flux, flow direction, inlet subcooling, inlet throttling, heated length-to-diameter ratio and natural circulation. The test data are compared with those of the authors' previous experiments with different test sections and existing correlations.

1.0 INTRODUCTION

The critical heat flux (CHF) condition constitutes an upper boundary of the efficient boiling heat transfer regime, and economic operation of heat transfer equipments can be achieved by designing them to operate near but not exceeding it. The CHF has been extensively investigated over the past three decades mainly with development of water-cooled nuclear reactors. Now many aspects of the phenomenon are well understood and several reliable correlations are available for most conditions. A number of excellent survey of the CHF are available in books [1-3] and papers[4-6].

However there are two major problems; one is insufficient understanding of the physical phenomena which results in too many empirical correlations, the other is the unbalance of study, i.e., concentration of works on the high pressure and high flow conditions related to commercial water cooled nuclear reactors. The former is expected to be solved through more experimental investigation and development of generalized correlations(Katto, 1985) or theoretical prediction methodologies. Considerable efforts should be also given to mitigate the latter problem.

The importance of CHF at low pressure and low velocity (LPLV) conditions is increasing in relation to the commercial nuclear reactors in accident conditions, the passive safety reactors, small-scale district heating reactors, etc. This leads to considerable studies for this specific area during the past

decade[7-15]. Korea Advanced Institute of Science and Technology (KAIST) is performing the LPLV CHF study in both experimental and theoretical aspects. Experiments with two round tube test sections ($D = 6$ mm and 8.8 mm) and some analytical work are already reported[16]. This work continues the previous work to improve overall understanding of the CHF phenomenon.

2.0 BACKGROUND

The CHF characteristics would be quite different at low pressure compared with high pressure conditions due to different water properties. Especially vapor-to-liquid specific volume ratio at 0.1 MPa is about 1600, which is 260 times that at 15 MPa. This is the primary reason that flow becomes less stable at low pressure. The large specific volume ratio also results in large bubbles and therefore different boiling characteristics in channels of relatively small diameter. Significant changes in surface tension and viscosity would also affect the behavior of the liquid-vapor interface. In addition to these pressure effects, low velocity makes the buoyancy effect significant. So the LPLV CHF is a complex phenomenon and systematic interpretation is difficult.

This characteristic of the LPLV CHF was recognized early and experimental work and correlation development have been performed since late 1950s. However it is only recently that this phenomenon is extensively studied. Correlation by Griffith et al. (modified Zuber correlation)[17] is the most famous one frequently used in nuclear reactor safety codes.

Considerable works have been reported for the present subject during the past decade. The most important and comprehensive works are those by Mishima et al.[7-10]. They performed a series of experiments for three different channel geometries: an internally heated annulus, two rectangular channels, and a round tube. Additional CHF experiments for LPLV conditions have been performed by other workers including Rogers et al.[11] for water flow in annuli, Sudo et al.[12, 13] for rectangular channels, El-Genk et al.[14] for annuli, Weber et al.[15] for a short round tube, and recently Chang et al.[16]. Important findings can be summarized as follows:

(a) The CHF at zero net flow occurs due to counter-current flow limitation (CCFL) (flooding or flow reversal), which is represented by the following correlation from the Wallis' flooding correlation (Wallis, 1969) :

$$G_{CF} = \frac{A}{A_h} \cdot \frac{C^2 h_{fg} \sqrt{\rho_g g \Delta \rho D}}{[1 + (\rho_g / \rho_f)^{1/4}]^2} \quad (1)$$

It generally gives much lower CHF value than the pool-boiling CHF. The flooding could be the cause of CHF even in the non-zero flow condition as long as countercurrent flow is established in the boiling channel. Chang et al.(1991) derived the following implicit

form of flooding-limited CHF for non-zero flow condition.

$$q_{CHF} = \frac{(A/A_h) C^2 h_{fg} (\rho_g g \Delta \rho D)^{1/2}}{1 + (\rho_g/\rho_f)^{1/4} [1 - (A/A_h) (h_{fg} G/q_{CHF})]^{1/2}} \quad (2)$$

However the constant C varies significantly according to the test section geometry including dimension.

(b) The CHF at LPLV conditions is lower than that predicted by conventional low-velocity CHF correlations. The CHF as a function of mass flux shows different behavior between the round tube and the other channel geometries with unheated wall. The CHF is generally higher in round tubes.

(c) At intermediate mass velocities the CHF is significantly affected by flow instabilities under low pressure. Downward flow is more susceptible to the instability and therefore has lower CHF value than upward flow. Downflow CHF is affected by the inlet subcooling, inlet throttling, and upstream compressibility more than the upflow CHF.

(d) Flooding, churn-to-annular flow transition, dryout of liquid film surrounding the vapor plug in slug flow, and dryout of liquid film from annular flow are considered as the possible CHF mechanisms under LPLV conditions.

Frequently the CHF at LPLV conditions is analyzed using the following dimensionless parameters:

$$G^* = G/\sqrt{\lambda \rho_g g \Delta \rho} \quad (3)$$

$$g^* = q/(h_{fg} \sqrt{\lambda \rho_g g \Delta \rho}) \quad (4)$$

$$D^* = D/\lambda \quad (5)$$

where

$$\lambda = \sqrt{\sigma/g \Delta \rho} \quad (6)$$

3.0 EXPERIMENTAL APPARATUS AND PROCEDURE

3.1 Experimental Loop

The experimental loop, which is almost the same as that used in the previous experiments[16], is schematically shown in Fig. 1. Please refer to Chang et al.[16] for more detailed information on the loop and test procedure.

3.2 Test Section

The test section was made up of 10 mm-i.d. and 2 mm-thick Type-304 stainless steel tube with variable heated length of 0.9 m and 0.6 m as shown in Fig. 2. A copper electrode is welded to each end of the test section to deliver the electric power from a 32V, 2000A DC power supplier. To observe tube wall temperature variation, 14 Chromel-Alumel (Type K) thermocouples are spot-welded onto the outside of the stainless steel tube. The test section tube and copper electrode is electrically insulated from the other parts of the loop by teflon bushings.

3.3 Instrumentation and Data Processing

The test section wall temperatures were detected by Type-K thermocouples, and processed, stored and displayed by a data acquisition system consisting of a HP3852A Data Acquisition/Control Unit, a HP Series 300 Workstation and a Keithley System 740 scanning thermometer. The water (or steam) temperature at the inlet and outlet of the test section was detected by Type-T thermocouples and displayed with an Omega Model 2176A digital indicator.

Test section pressure was measured by a bourdon-type pressure gauge and confirmed by estimation based on hydrostatic head below the overhead tank water level. The pressure at test section outlet was estimated to be 110 kPa. The flow rate into the test section was measured by a rotameter assembly covering a range from 0.01 to 2.5 liter/min.

The critical heat flux condition was defined as the condition where maximum wall temperature exceeded 300 °C with a trend of rapid increase (Fig. 3). Practically use of different set point did not give significant difference in resulted CHF values. The heat flux was calculated from the power input to the test section and known heated area assuming uniform heat flux. The test section power was determined from the current and resistance considering the effect of temperature variation.

The uncertainties of the final CHF data were estimated by incorporating the contribution of each independent variable affecting the parameter. The estimated uncertainties are as follows:

- test section outlet pressure: ± 1 kPa
- inlet subcooling: ± 5 kJ/kg
- mass flux: ± 5 %
- heat flux: ± 4 %

4.0 RESULTS AND DISCUSSION

Total of 232 CHF data were obtained with varying flow direction, inlet conditions (mass flux, subcooling and throttling) including natural circulation conditions. Downward flow test without inlet

throttling was limited to the very low flow region because stable flow could not be established at higher flow.

4.1 Overall Behavior of CHF

The overall behavior of CHF as a function of mass flux is shown in Fig. 4 for the stable flow condition where flow excursion is avoided and flow oscillation is not large. Here the positive and negative mass flux denote upflow and downflow, respectively. Zero mass velocity means complete bottom blockage or zero net flow at test section inlet. Figure 5 shows the variation of thermodynamic quality at tube exit, based on the inlet flow condition and heat input, under CHF condition.

Overall behavior was very similar to that previously observed by the authors[16] and can be summarized as follows:

(a) The CHF monotonously increased with mass flux from a minimum value at zero inlet mass flux.

(b) The critical quality generally decreased and merged to a line as mass flux is increased. There was a transition point in the trend of critical quality near $G = 10 \text{ kg/m}^2\text{s}$, which corresponds to the transition of CHF mechanism from flooding to liquid film dryout.

(c) The stable CHF was almost the same for given mass flux regardless of flow direction, inlet subcooling and inlet throttling.

(d) The CHF was a decreasing function of L_h/D for given D .

(e) The location of CHF occurrence moved from the bottom to the top (exit) of the test section, as the upward flow rate was increased from zero. The CHF always occurred at the tube exit for flow rate greater than a threshold value.

4.2 Parametric Effects on the CHF Data

Now let us briefly examine the parametric effects found in our experimental data. Note that discussion is limited to the stable flow condition.

Effect of mass flux. The CHF monotonously increased as mass flux is increased from zero regardless of the flow direction, inlet subcooling, and inlet throttling for stable flow condition. The trend was almost linear in the lower flow region except near-zero flow, but the rate of increase decreased in the higher flow region. The behavior of CHF at very low flow is discussed later.

Effect of flow direction. When large inlet throttling was provided, the downflow CHF was generally lower than the upflow CHF with a difference less than 10% (see Fig. 6). In case of no inlet

throttling, downward flow was much more susceptible to the instabilities and premature CHF due to flow excursion could occur.

Effect of inlet subcooling. The effect of inlet subcooling was negligible in our experimental range (Fig. 7). It has been suggested as a useful measure in defining the low flow region under low pressure (Chang et al., 1991).

Effect of inlet throttling. Throttling just before the inlet of a boiling channel under low pressure increases the stability of flow, and therefore generally increases the CHF. Its effect on the CHF was negligible in the very low flow region, i.e., the flooding-limited CHF region. It was relatively small in upward flow but significant for downflow condition so that even a stable flow condition could not be established without inlet throttling.

Effect of heated length-to-diameter ratio. In case of the same inlet condition, the CHF in the shorter tube was 40 - 50% higher than that in the longer tube. This observation indicates that CHF is proportional to L_h^a ($a = 0.8$ to 1.0) for the same diameter tube.

Natural circulation effect. The CHF appeared to be considerably small in natural circulation condition compared with forced circulation. This does not agree to the findings by Mishima and Ishii[7] for an annulus.

4.3 Further Discussions

The behavior of CHF at very low upward flow is illustrated by Figs. 9 and 10. The trend of CHF and critical quality indicate that there is a threshold mass flux at which the CHF mechanism changes. This threshold corresponds to the maximum mass flux for flooding CHF previously derived by the authors (Chang et al., 1991) as shown in Fig. 10. This is clearly confirmed by the location of CHF occurrence. However it should be noted here that the value of C (0.77 and 0.65 for the longer and shorter tubes, respectively) in Eqs. (1) and (2) was found to be considerably lower than that observed by Mishima and Nishihara[8] ($C = 1.66$) and Chang et al.[16] ($C = 1.27$ for TS-1 and 0.98 for TS-2).

The present CHF data are compared with the previous results by authors (TS-1: $D = 6\text{mm}$, $L_h = 0.72\text{m}$, $t = 1\text{mm}$; TS-2: $D = 8.8\text{mm}$, $L_h = 0.72\text{m}$, $t = 0.6\text{mm}$) in Fig. 11. This shows that the CHF is a decreasing function of length-to-diameter ratio. Figure 12 shows the CHF as a function of the local thermodynamic quality to check the potential of local condition type correlation for the LPLV region. Excluding the data for very low CHF (which is related to flooding-limited CHF), the CHF data for each heated length lies on a single curve approaching the point ($X_c = 1.0$, CHF = 0). The CHF is considered to be affected by length-to-diameter ratio as well as diameter. The CHF in TS-2 seems to be somewhat particular compared with others, probably due to very small tube thickness. As a conclusion, a quality-based correlation seems to be feasible if the effect of heat length is incorporated and the

flooding-limited CHF for near zero flow condition is properly treated.

Figure 13 compares the present experimental data with predictions by several existing correlations. Chang et al. correlation predicts well the data of the longer test section but not well for the shorter test section. This implies the need for improvement of the correlation, especially for the effect of length-to-diameter ratio. Most other correlations considerably overpredicts the CHF.

5.0 CONCLUSION

Important findings of this work are summarized as follows:

(a) Most findings by previous workers (especially by Mishima et al. and Chang et al.) on the LPLV CHF were confirmed in the present experiments.

(b) The CHF appeared to be lower in natural circulation condition compared with forced circulation condition, contrary to the finding of Mishima and Ishii (1982) for an annulus. This effect should be further studied.

(c) The constant C in Wallis flooding correlation was found to be much lower in the present test section. The effect of tube diameter on C should be clarified through more experiments.

(d) The quality-based CHF correlation for the LPLV CHF seems to be promising if the effect of length-to-diameter ratio and contribution of flooding are properly incorporated.

NOMENCLATURE

A	flow area of a channel	m^2
A_h	heated surface area	m^2
C	constant in Wallis correlation for flooding	-
D	diameter	m
D^*	dimensionless diameter	-
G	mass Flux	kg/m^2s
G^*	dimensionless mass flux	-
g	gravitational acceleration	m/s^2
h_{fg}	latent heat of vaporization	kJ/kg
L_h	channel heated length	m
P	pressure	kPa
q_c	critical heat flux	kW/m^2
q_{cF}	flooding-limited CHF	kW/m^2
q'	dimensionless heat flux;	-
X_c	critical quality	-

Greek Symbols

l	Taylor wave length	m
r	density	kg/m^3
Dr	density difference between liquid and vapor	kg/m^3

s phases
s surface tension

N/m

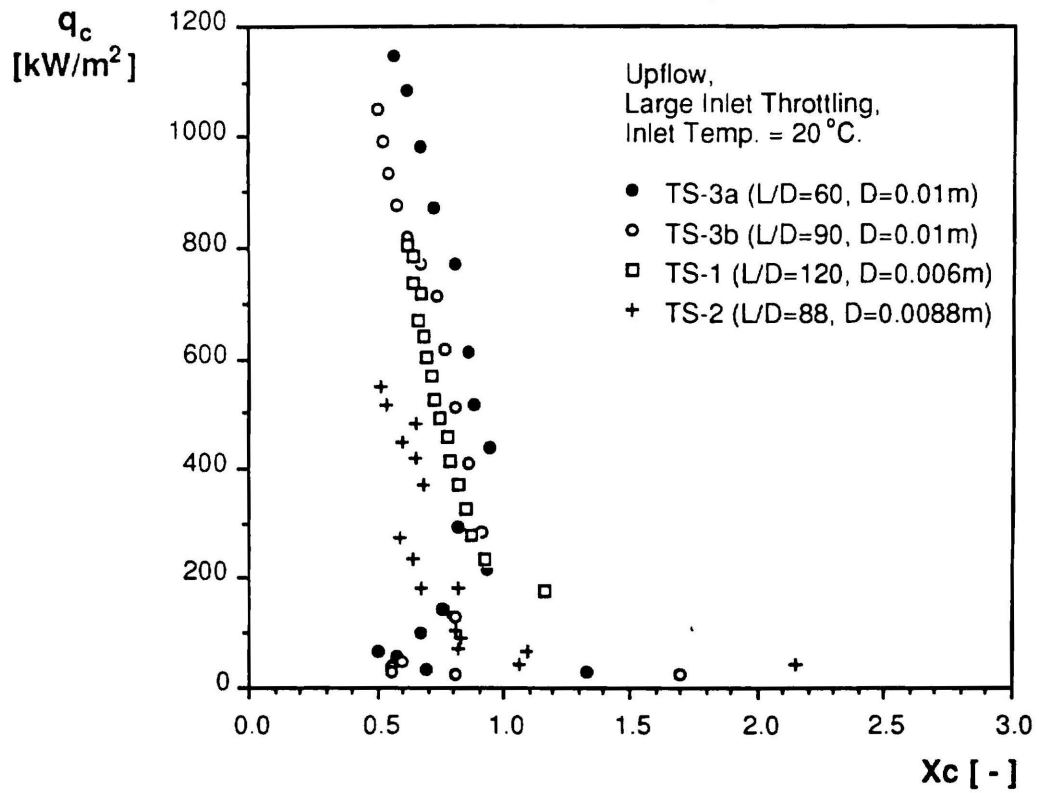
Subscripts

f saturated liquid
g saturated vapor
fg difference between saturated liquid and vapor phases

REFERENCES

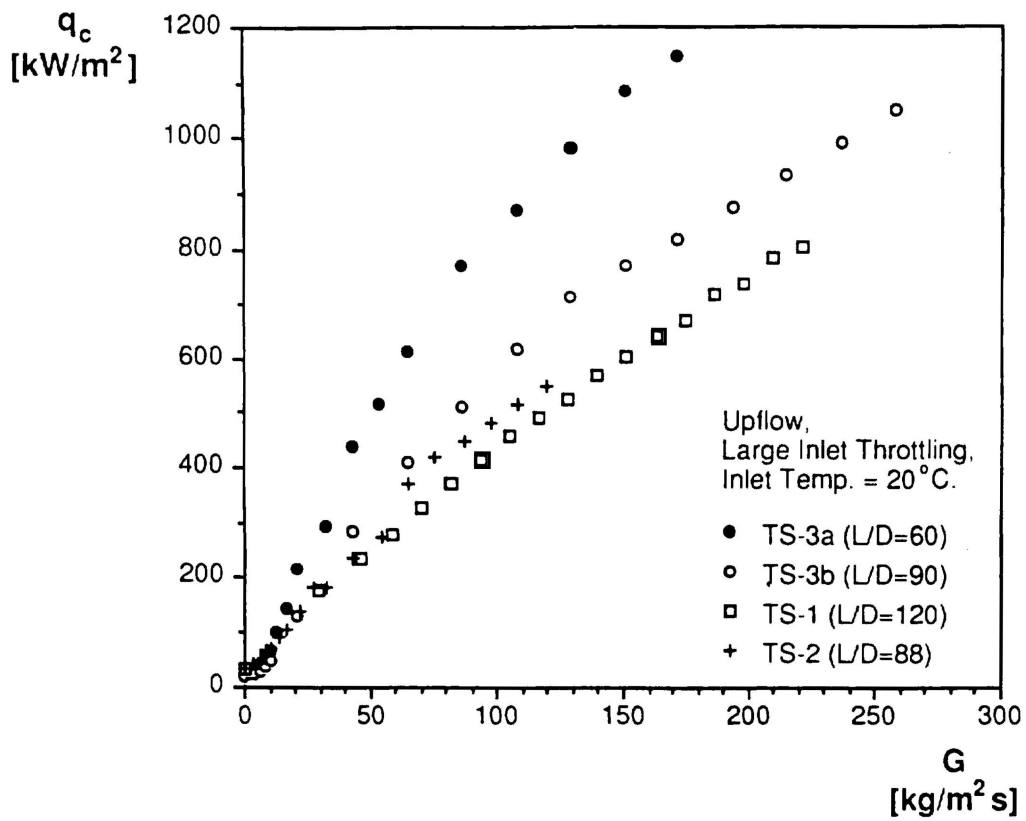
- (1) Collier, J.G., Convective Boiling and Condensation, 2nd ed., McGraw-Hill, New York, pp. 248-313, 1981.
- (2) Hewitt, G.F., "Burnout," Handbook of Multiphase Systems, G. Hetsroni, ed., Hemisphere, Washington, D.C., pp. 6.66-6.141, 1982.
- (3) Katto, Y., "Critical heat flux," Advances in Heat Transfer, Vol. 17, Academic Press, London, pp. 1-64, 1985.
- (4) Bergles, A.E., "Burnout in Boiling Heat Transfer, Part II: Subcooled and Low-Quality Forced Convection Systems," Nucl. Safety, Vol. 18, 154-167, 1977.
- (5) Bergles, A.E., "Burnout in Boiling Heat Transfer, Part III: High-Quality Forced Convection Systems," Nucl. Safety, Vol. 20, 671-689, 1979.
- (6) Theofanous, T.G., "The Boiling Crisis in Nuclear Reactor Safety and Performance," Int. J. Multiphase Flow, Vol. 6, 69-95, 1990.
- (7) Mishima, K. and Ishii, M., "Experimental Study on Natural Convection Boiling Burnout in an Annulus," Proc. 7th Int. Heat Transfer Conf., Munich, Vol. 4, Paper No. FB 23, 1982.
- (8) Mishima, K. and Nishihara, H., "The Effect of Flow Direction and Magnitude on CHF for Low Pressure Water in Thin Rectangular Channels," Nucl. Eng. Des., Vol. 86, 165-181, 1985.
- (9) Mishima, K. and Nishihara, H., "Effect of Channel Geometry on Critical Heat Flux for Low Pressure Water," Int. J. Heat Mass Transfer, Vol. 30, 1169-1182, 1987.
- (10) Mishima, K., Nishihara, H. and Michiyoshi, I., "Boiling Burnout and Flow Instabilities for Water Flowing in a Round Tube Under Atmospheric Pressure," Int. J. Heat Mass Transfer, Vol. 28, 1115-1129, 1985.
- (11) Rogers, R.T., Salcudean, M. and Tahir, A.E., "Flow Boiling Critical Heat Fluxes for Water in a Vertical Annulus at Low Pressure and Velocities," Proc. 7th Int. Heat Transfer Conf., Munich, Vol. 4 (1982) Paper No. FB 28, 1982.

- (12) Sudo, Y. and Kaminaga, M., "A CHF Characteristic for Downward Flow in a Narrow Vertical Rectangular Channel Heated from Both Sides," *Int. J. Multiphase Flow*, Vol. 15, 755-766, 1989.
- (13) Sudo, Y., Miyata, K., Ikawa, H., Kaminaga, M. and Ohkawara, M., "Experimental Study of Differences in DNB Heat Flux between Upflow and Downflow in Vertical Rectangular Channel," *J. Nucl. Sci. Tech.*, Vol. 22, 604-618, 1985.
- (14) El-Genk, M.S., Haynes, S.J. and Kim, S.H., "Experimental Studies of Critical Heat Flux for Low Flow of Water in Vertical Annuli at Near Atmospheric Pressure," *Int. J. Heat Mass Transfer*, Vol. 31, 2291-2304, 1988.
- (15) Weber, P. and Johannsen, K., "Study of the Critical Heat Flux Condition at Convective Boiling of Water: Temperature and Power Controlled Experiments," *Proc. 9th Int. Heat Transfer Conf.*, Jerusalem, Vol. 2, 63-68, 1990.
- (16) Chang, S.H., Baek, W.-P., and Bae, T.M., "A Study of Critical Heat Flux for Low Flow of Water in Vertical Round Tubes Under Low Pressure," *Nucl. Eng. Des.* Vol. 132, 225-237, 1991.
- (17) Griffith, P., Avedisian, C.T. and Walkush, J.P., "Counterflow Critical Heat Flux," *AIChE Symp. Ser.*, No. 174, Vol. 74, 147-155, 1978.



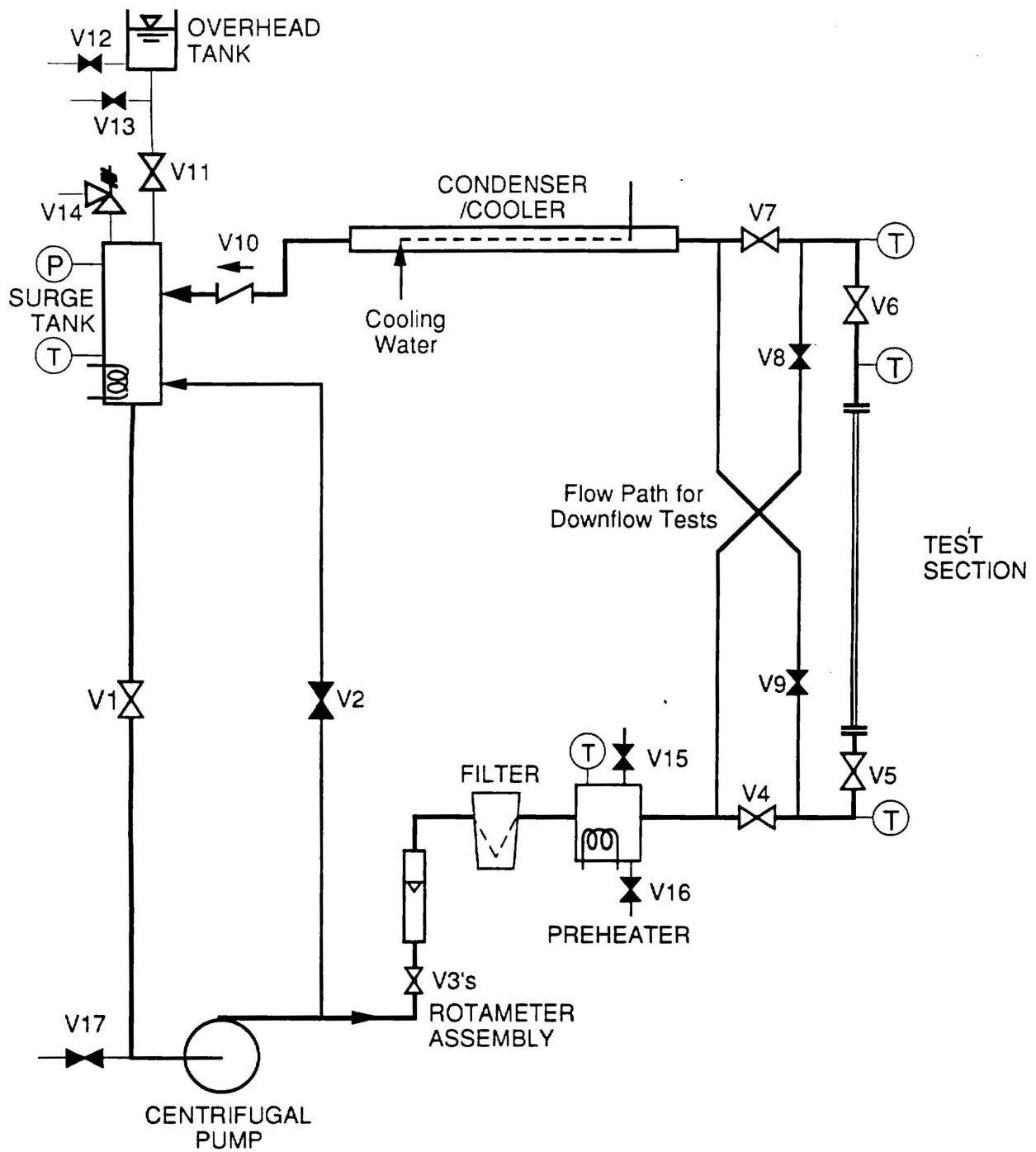
[CHF versus Critical Quality]

FIG. 12



[Comparison of present data with previous KAIST experiments]

FIG. 11



[Schematic of the Experimental Loop]
 FIG. 1

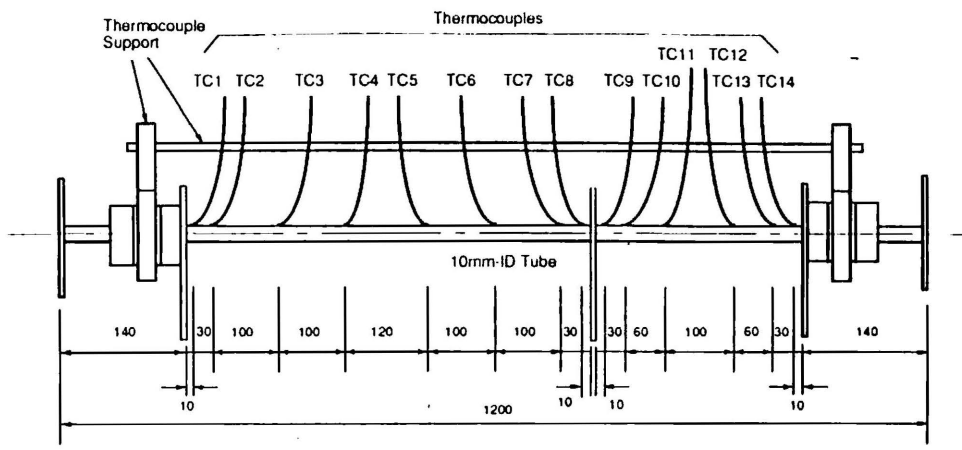
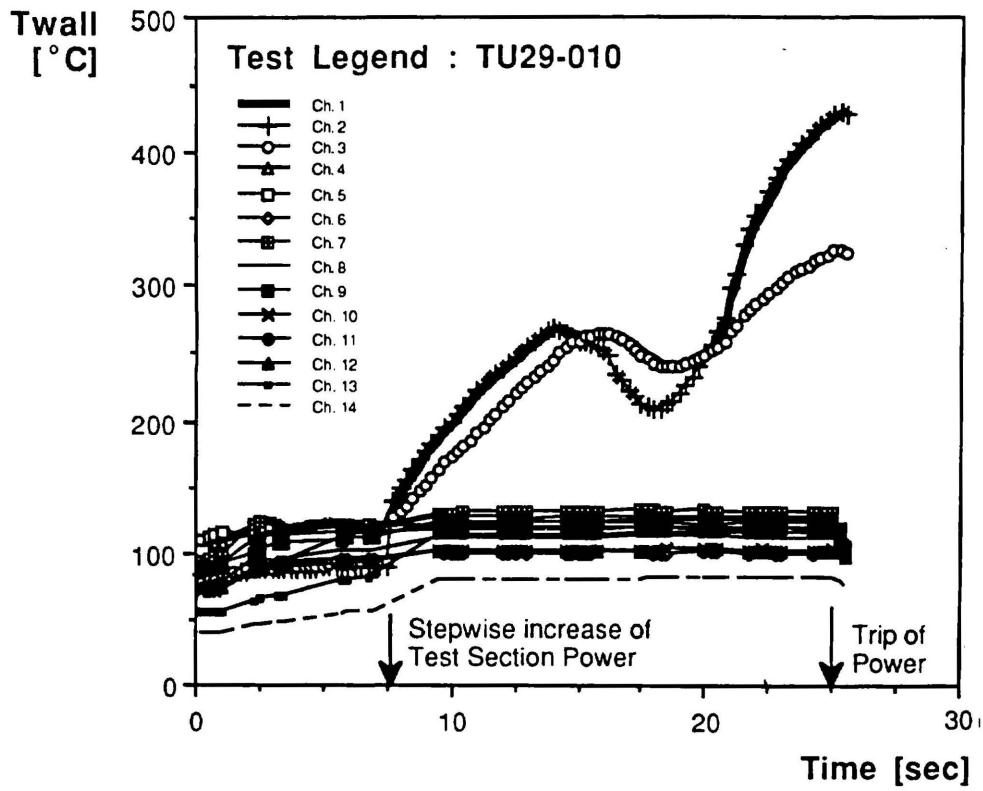
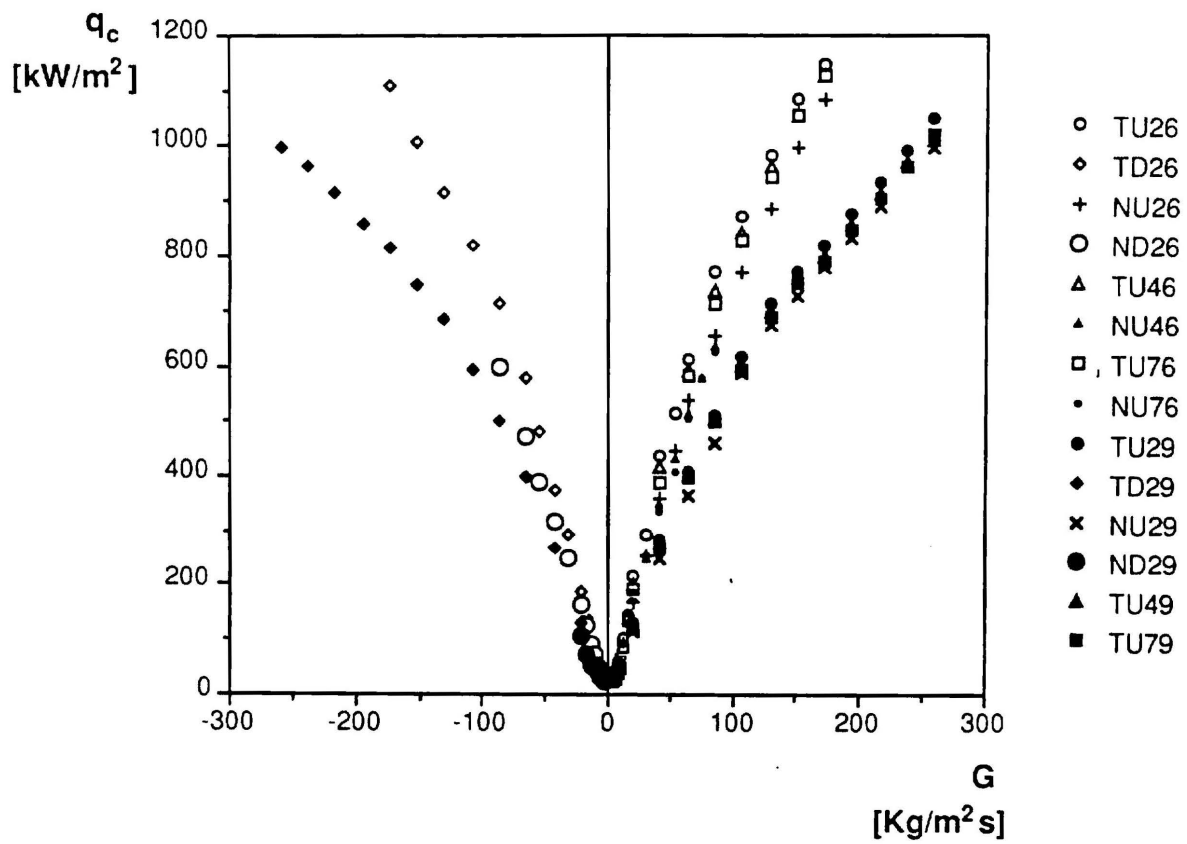


Fig. 2 Test Section-3 (TS-3)



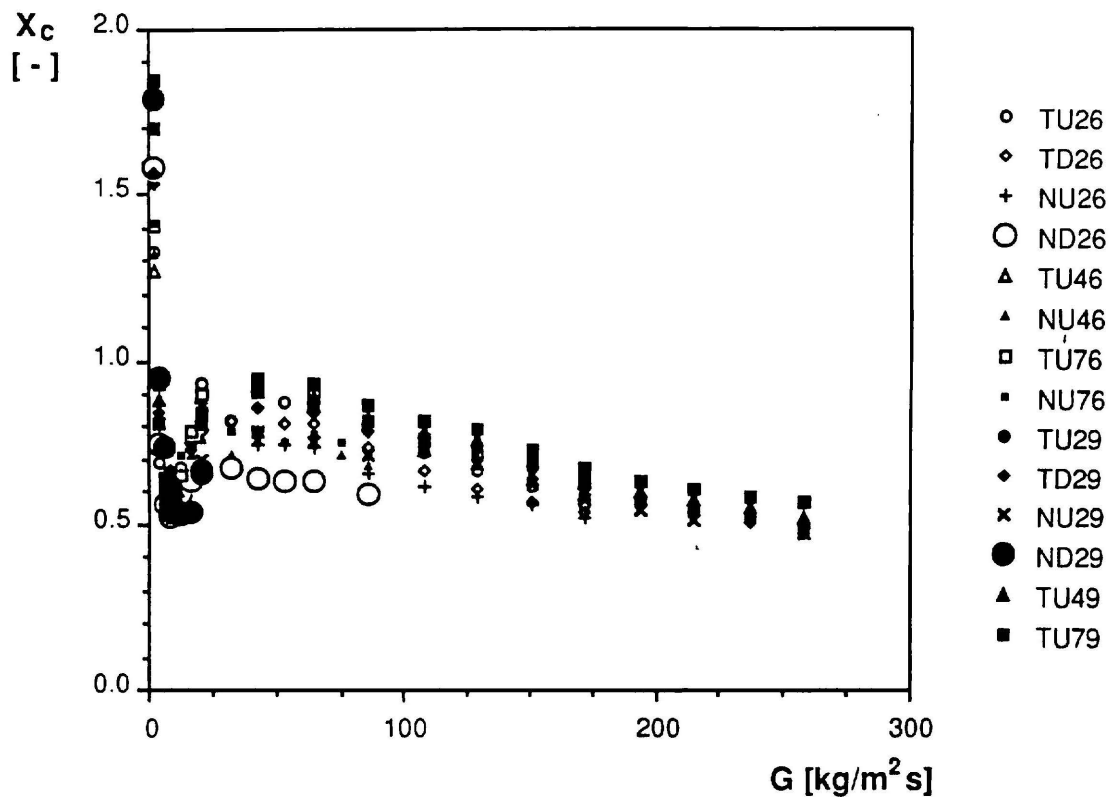
[Wall Temperature Variation Near the CHF]

FIG. 3



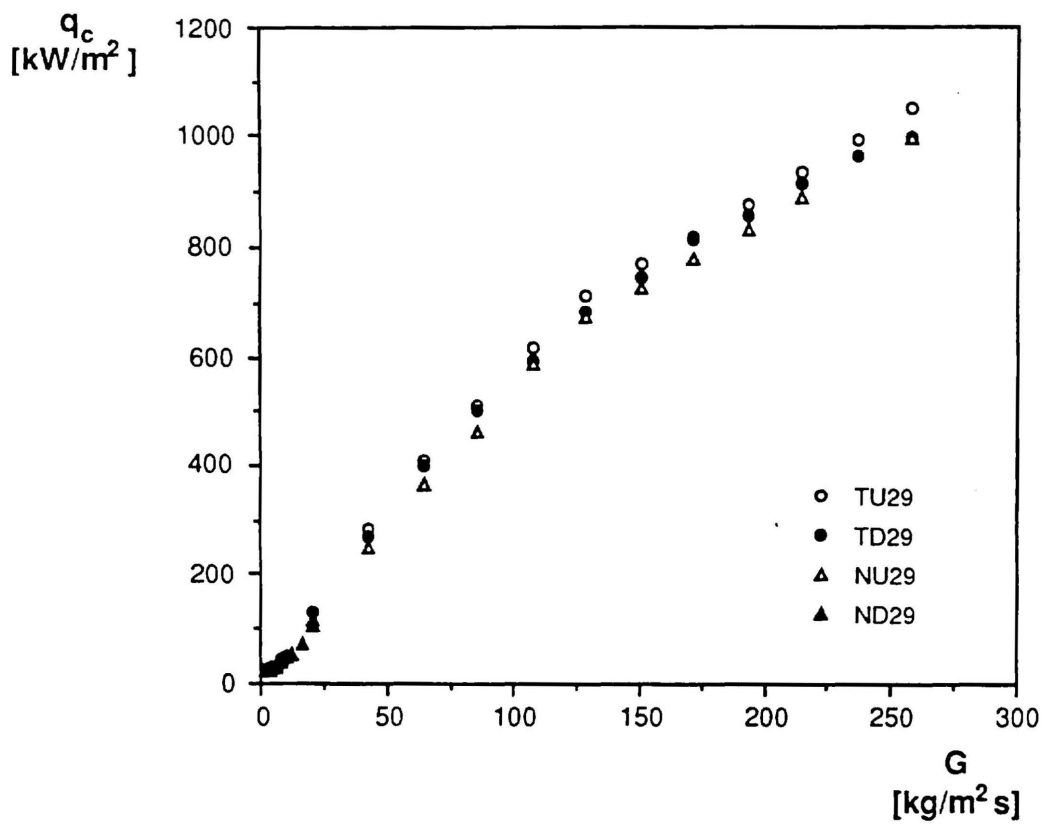
[Overall Behaviour of CHF]
 (CHF vs. Mass Flux)

FIG. 4

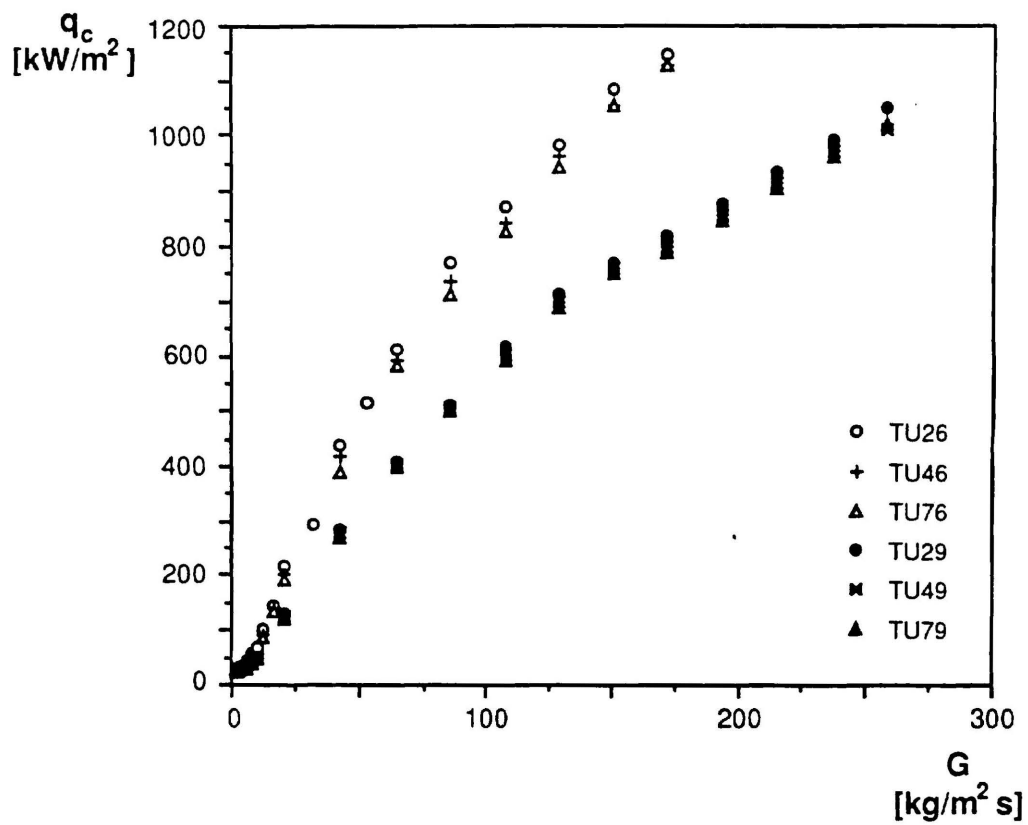


[Critical Quality vs. Mass Flux]

F14.5

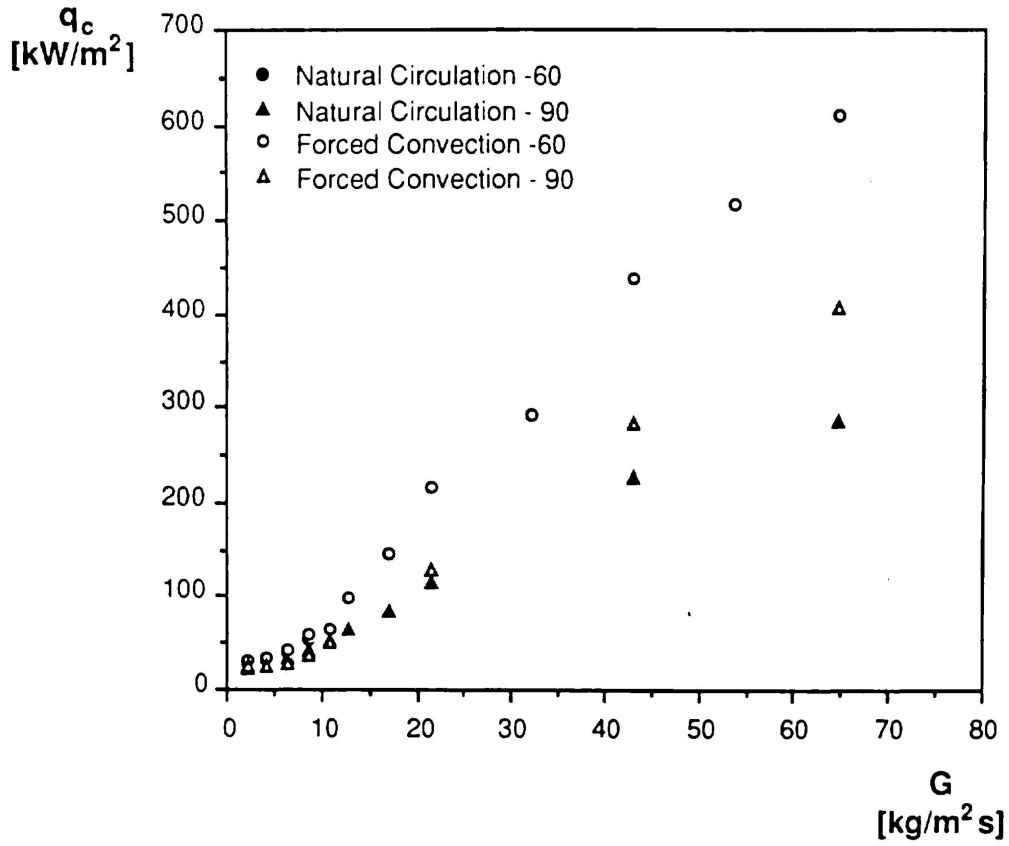


[Effect of Flow Direction]
 FIG. 6



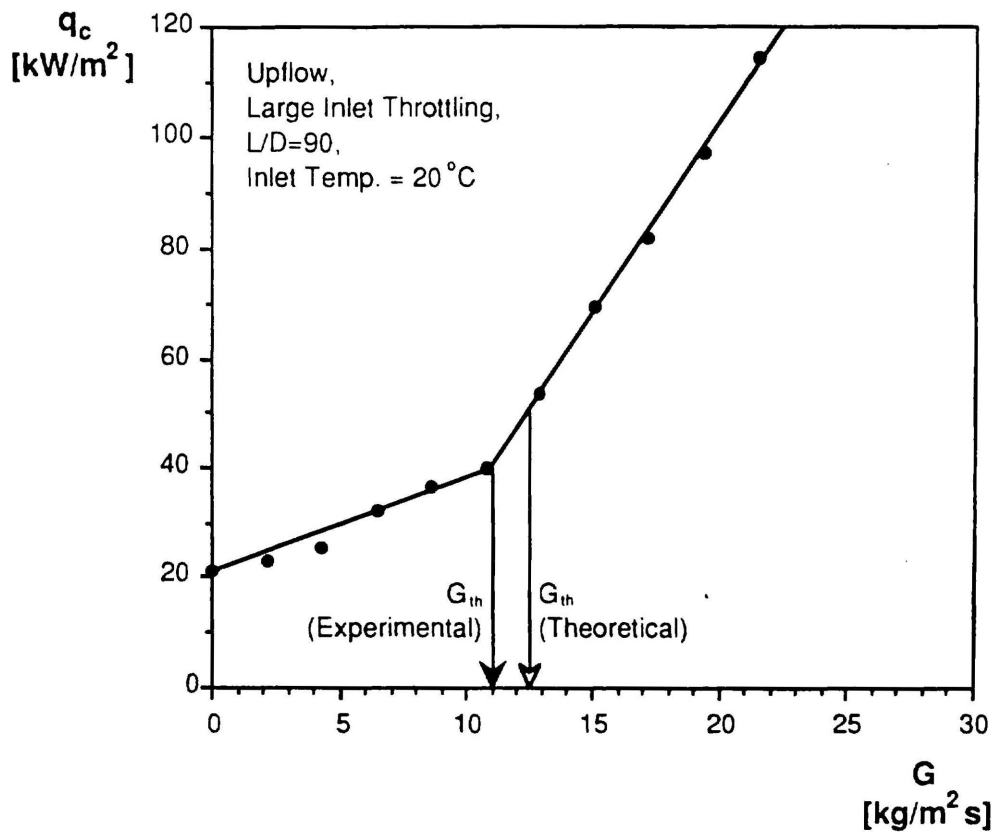
[Effect of Inlet Subcooling]

FIG. 7



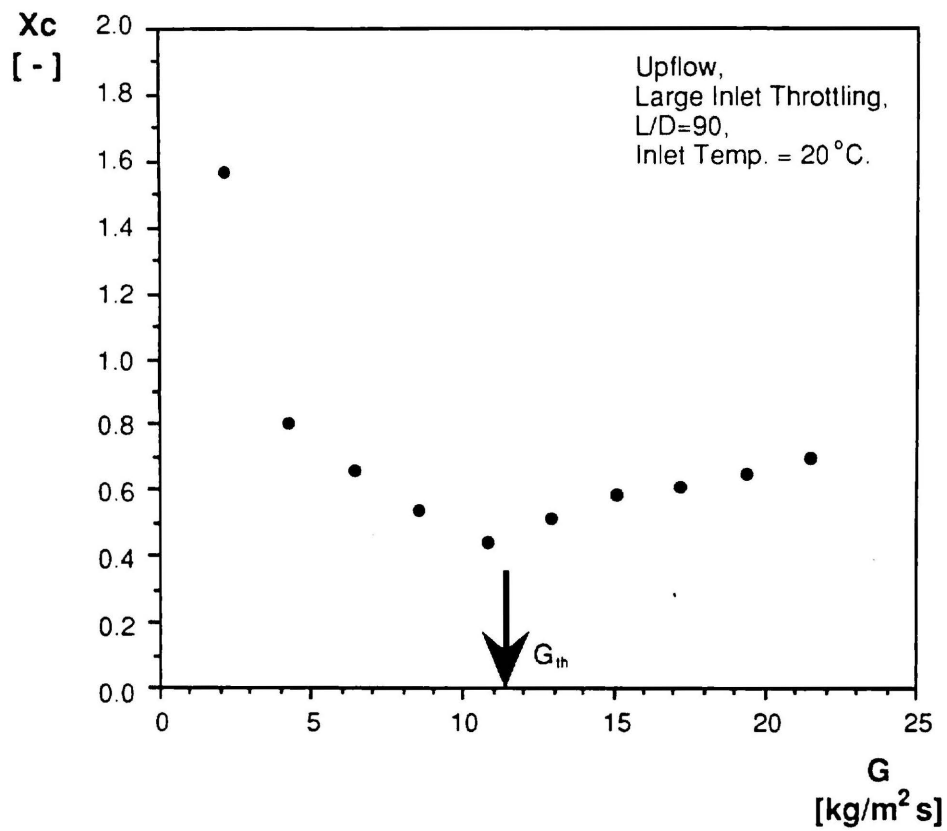
[Effect of Natural Circulation on the CHF]

FIG.8



[CHF at Very Low Flow]

FIG. 9



[Critical Quality at Very Low FLOW]

FIG. 10

